Article

Iron(II)/(NH)P Macrocycles: Modular, Highly Enantioselective Transfer Hydrogenation Catalysts

Raphael Bigler, Raffael Huber, Marco Stöckli, and Antonio Mezzetti

ACS Catal., **Just Accepted Manuscript** • DOI: 10.1021/acscatal.6b01872 • Publication Date (Web): 23 Aug 2016

Iron(II)/$(NH)_2P_2$ Macrocycles: Modular, Highly Enantioselective Transfer Hydrogenation Catalysts

*Raphael Bigler, Raffael Huber, Marco Stöckli, and Antonio Mezzetti**

Department of Chemistry and Applied Biosciences, ETH Zürich, CH-8093 Zürich, Switzerland

ABSTRACT: A generalized protocol for the synthesis of chiral $(NH)_2P_2$ macrocycles allows changing the linker between the phosphines and gives access to a family of such ligands, as demonstrated for the propane-1,3-diyl analogue. The corresponding complexes based on earth-abundant and nontoxic iron were applied as catalysts in the asymmetric transfer hydrogenation of polar double bonds. Thanks to the ligand modularity and to the use of tunable isonitriles as ancillary ligands, the catalyst system can be individually optimized for each substrate to give high enantioselectivity (up to 99.9% conversion and 99.6% ee, TOF up to >3 950 h^{-1}) for a broad scope of 26 substrates.

KEYWORDS: alcohols, asymmetric catalysis, hydrogen transfer, iron, macrocyclic ligands

INTRODUCTION

The asymmetric reduction of prochiral ketones, imines, and olefins is the most important metal-catalyzed enantioselective reaction in industry. However, the high cost of the involved transition

metals, primarily ruthenium, rhodium, and iridium, together with that of the chiral ligands, has hampered the application of such precious metal-based catalysts.[1] Thus, production processes relying on asymmetric reduction are still scarce. Recently, cheap, non-toxic, and environmentally benign iron catalysts have emerged as an attractive alternative to precious metals for the reduction of polar double bonds, i.e. ketones and imines (Chart 1).[2-7]

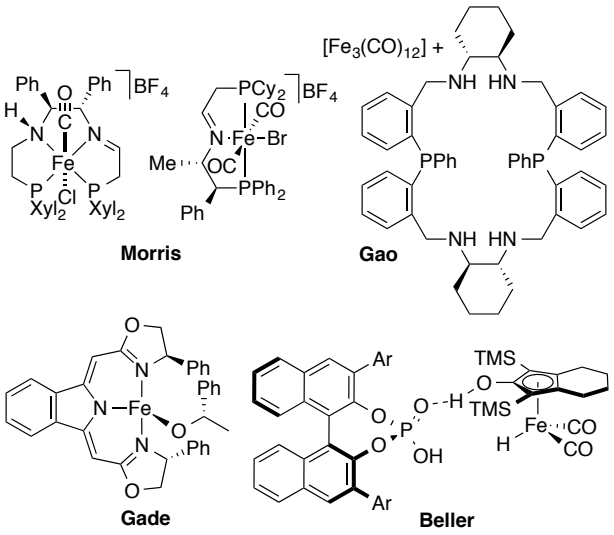

Chart 1. Iron-based Catalysts for Asymmetric Reduction

Most prominently, Morris has developed a series of highly active iron(II)/P(NH)NP and PNP precatalysts, but the enantioselectivity is modest for most substrates.[3] On the other side, the catalyst systems developed by Gao,[4] Gade,[5] and Beller[6] are generally highly enantioselective, but the turnover frequencies and numbers are low in most cases. Thus, the development of base metal catalysts that are both highly active and enantioselective is still a formidable challenge.

Recently, we developed the macrocyclic iron(II) bis(isonitrile) complexes Λ-*cis*-*β*-$[Fe(CNR)_2((S_P,S_P,S_C,S_C)$-**1a**$)](BF_4)_2$ (R = CEt_3, **2a**; R = N^iPr_2, **2b**), which are the first well-defined iron-based precatalysts that combine high activity (TOF up to 6 650 h^{-1}, TON up to 10 000) and enantioselectivity (up to 99% ee) for a broad scope of aryl alkyl ketones under asymmetric

transfer hydrogenation (ATH) conditions (Chart 2).[7] In complexes **2a** and **2b**, the chiral information stems from the C_2-symmetric tetradentate $(NH)_2P_2$ macrocycle (S_P,S_P,S_C,S_C)-**1a**. Sterically and electronically tunable isonitriles are required as ancillary ligand to stabilize the catalyst and to increase the enantioselectivity to >95% ee for most substrates.[7b] The scope of the ATH reaction includes standard acetophenone derivatives, but also challenging or industrially relevant substrates such as *tert*-butyl phenyl ketone[8] or 3,5-bis(trifluoromethyl)acetophenone[9] are efficiently reduced (99% conversion, 97% and 98% ee, respectively).

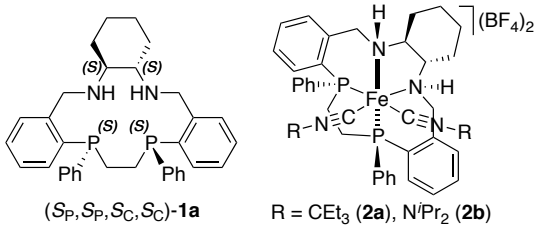

(S_P,S_P,S_C,S_C)-**1a** R = CEt_3 (**2a**), N^iPr_2 (**2b**)

Chart 2. Macrocyclic Iron(II)/$(NH)_2P_2$ Complexes

Although the enantioselectivity was high for most substrates, there is room for improvement with some ketones, particularly acyl heterocycles (90–98% ee) and other substrates such as 3-trifluoromethylacetophenone (96% ee), an important intermediate in the synthesis of fungicides.[10] As further optimization of the ancillary isonitriles (*C*-isonitrile $CNCEt_3$ in **2a** and *N*-isonitrile CN^iPr_2 in **2b**, respectively) was not successful,[7b,11] we decided to turn our attention to the macrocyclic $(NH)_2P_2$ ligand **1a**. A careful analysis of the crystal structures of the analogous bis(isonitrile) complexes **2c**-**2e** bearing 1-adamantyl (**2c**), *tert*-butyl (**2d**), and phenyl isonitriles (**2e**) as ancillary ligands shows that the five-membered P–Fe–P chelate ring is flexible and adopts different half-chair conformations. Depending on the isonitrile ligand, the P–C–C–P torsion angle involved in the ethane-1,2-diyl bridge changes from +20.7(5)° in **2d** to –37.5(4)° in **2e**.[7b] We speculated that a more rigid chelate ring may lead to higher enantioface discrimination, as

the macrocycle might be less prone to rearrange to accommodate the substrate in the energetically disfavored transition state leading to the minor enantiomer of the secondary alcohol product.

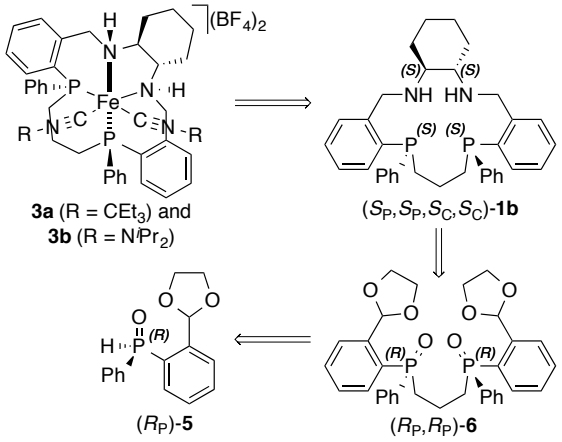

Scheme 1. Retrosynthetic Analysis of Complexes 3a and 3b

A possible strategy to access more enantioselective catalysts might therefore rely on the incorporation of a more rigid P–Fe–P chelate ring, and we planned to tackle this challenge by introducing a propane-1,3-diyl (–$(CH_2)_3$–) bridge between the phosphorus donors, as a six-membered chelate ring is expected to be less flexible than the five-membered P–Fe–P chelate ring in the ethane-1,2-diyl (–$(CH_2)_2$–) linker of the bis(isonitrile) complexes **2**. The synthesis of the 15-membered ring analogue seemed feasible with our recently developed, versatile procedure for the synthesis of $(NH)_2P_2$ macrocycles (Scheme 1).[7c] Instead of the methylation/oxidative coupling sequence from (R_P)-**5** that gives the ethane-1,2-diyl bridge in the parent ligand (S_P,S_P,S_C,S_C)-**1a** (Chart 2), we planned to use an alkylative dimerization with 1,3-diiodopropane to afford the propane-1,3-diyl-bridged diphosphine oxide (R_P,R_P)-**6**.[12] Enantiomerically pure (R_P)-**5** was previously accessed from Han's *H*-phosphinate (R_P)-**4** in one step and is also accessible as the S_P enantiomer.[7c,13,14]

Herein, we describe the synthesis of the 15-membered $(NH)_2P_2$ macrocycle (S_P,S_P,S_C,S_C)-**1b** containing a propane-1,3-diyl bridge and of the corresponding bis(isonitrile) iron(II) complexes $[Fe(CNR)_2((S_P,S_P,S_C,S_C)$-**1b**$)](BF_4)_2$ (**3**), which were assayed in the ATH of prochiral ketones and imines. The results described below highlight the versatility of the synthetic protocol for the preparation of $(NH)_2P_2$ macrocycles and the drastic effects of the bridge length between the phosphorus donors on the catalysis outcome. Even more importantly, they open the way to the development of a versatile family of ligands and catalysts.

RESULTS AND DISCUSSION

General Strategy. As outlined in Scheme 1, the synthesis of bis(isonitrile) iron(II) complexes **3** relies on the preparation of the $(NH)_2P_2$ macrocycle (S_P,S_P,S_C,S_C)-**1b**, which can be accessed by macrocyclization of the dialdehyde (S_P,S_P)-**7** with (1*S*,2*S*)-cyclohexane-1,2-diamine followed by reduction of the imine moieties. Dialdehyde (S_P,S_P)-**7** can be obtained by double stereoselective phosphine oxide reduction and acetal cleavage from diphosphine oxide (R_P,R_P)-**6** (Scheme 2). As mentioned above, the synthesis of the key intermediate (R_P,R_P)-**6** was planned by alkylative dimerization of the previously described enantiomerically pure secondary phosphine oxide (R_P)-**5** with 1,3-diiodopropane.[7c,12]

Synthesis of Dialdehyde (S_P,S_P)-7. Following our previous report,[7c] the secondary phosphine oxide (R_P)-**5** was prepared as a single enantiomer (99% ee) by treatment of Han's *H*-phosphinate (R_P)-**4**[13a] with an excess of (2-(1,3-dioxolan-2-yl)phenyl) lithium. To install the propane-1,3-diyl bridge between the phosphorus atoms, (R_P)-**5** was deprotonated with *n*-BuLi at –78 °C and treated with 1,3-diiodopropane (Scheme 2). After warming to room temperature overnight and purification by flash column chromatography, the desired diphosphine oxide (R_P,R_P)-**6** was

isolated in 89% yield as a single diastereoisomer (d.r. > 95:5). In contrast, the analogous reaction with 1,2-diiodoethane did not give the ethane-1,2-diyl-bridged analogue, which had to be prepared in a two-step procedure by methylation and oxidative coupling.[7c] The alkylative dimerization was also tested with 2,2-disubstituted 1,3-diiodopropanes $CR_2(CH_2I)_2$ (R = Me, Bn, fluorene-9,9-diyl). However, no conversion to the desired products was observed, which is ascribed to the *neo*-pentyl position of the leaving groups in these electrophiles.

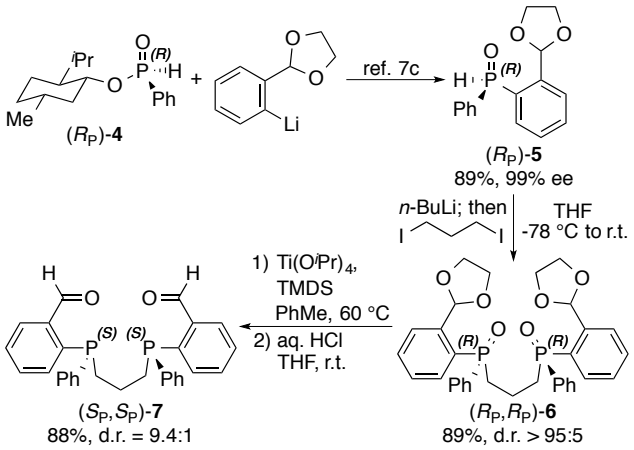

Scheme 2. Synthesis of Dialdehyde (S_P,S_P)-7

Treatment of (R_P,R_P)-**6** with Ti(O^{i}Pr)$_4$ and 1,1,3,3-tetramethyldisiloxane (TMDS) in hot toluene resulted in stereoselective reduction of the phosphine oxide moieties with *retention* of configuration at phosphorus. After work-up, the acetal protecting groups of the crude diphosphine were cleaved with aqueous hydrochloric acid. Purification by flash column chromatography afforded the desired dialdehyde (S_P,S_P)-**7** in 88% yield and as a 9.4:1 mixture of the *like* and the *meso* diastereoisomer. Overall, this synthetic route affords the propane-1,3-diyl-linked dialdehyde (S_P,S_P)-**7** in only four steps from Han's *H*-phosphinate (R_P)-**4** with an overall yield of 70%. As removal of the minor *meso* diastereoisomer either by recrystallization or column chromatography

was not possible, the dialdehyde (S_P,S_P)-**7** was used as a 9.4:1 mixture of diastereoisomers in the macrocyclization experiments (*vide infra*).

Synthesis of $(NH)_2P_2$ Macrocycle (S_P,S_P,S_C,S_C)-1b. The reaction of dialdehyde (*l*)-**7** with (*l*)-cyclohexane-1,2-diamine affords diastereomeric products and both enantiomers of the diamine have therefore to be studied individually. As for the ethane-1,2-diyl-bridged derivative, the macrocyclization experiments were carried out under high dilution conditions (0.01 M) to favor intra- over intermolecular imine formation in the second condensation step.[7e]

The $^{31}P\{^1H\}$ NMR spectrum of the reaction solution indicates that the reaction of (S_P,S_P)-**7** with (1*S*,2*S*)-cyclohexane-1,2-diamine gives exclusively the desired N_2P_2 macrocycle (Scheme 3). In contrast to the P–$(CH_2)_2$–P-linked N_2P_2 macrocycle, the propane-1,3-diyl analogue does not precipitate upon concentration. Therefore, the solvent was removed and the crude diimino N_2P_2 macrocycle (86% pure by $^{31}P\{^1H\}$ NMR spectroscopy) was directly reduced with $LiAlH_4$ in THF. After work-up, the desired $(NH)_2P_2$ macrocycle (S_P,S_P,S_C,S_C)-**1b** was obtained as a white solid in good yield and with acceptable purity (83% pure by $^{31}P\{^1H\}$ NMR spectroscopy).

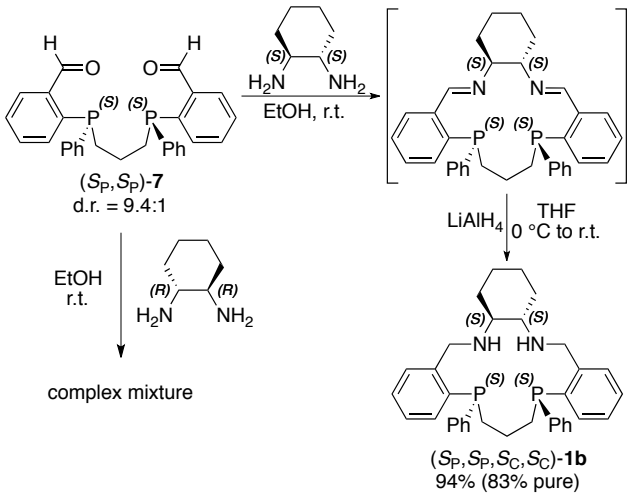

Scheme 3. Reaction of (S_P,S_P)-7 with (*l*)-Cyclohexane-1,2-diamine

In contrast to the reaction with (1*S*,2*S*)-cyclohexane-1,2-diamine, the reaction solution of (S_P,S_P)-**7** with the *R*,*R* enantiomer showed several signals with similar intensity that were assigned to oligomeric products. Attempts to employ acid catalysts,[7e] metal templates in analogy to Morris,[3f] or more dilute conditions failed to give a macrocyclic product.

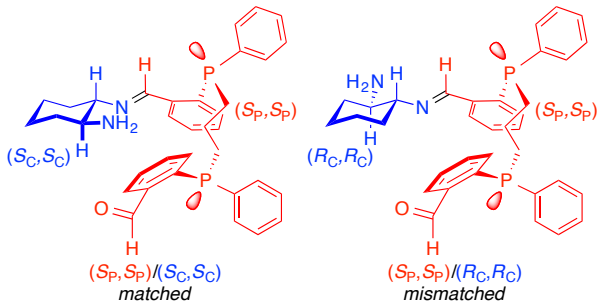

Chart 3. Conformational Analysis of the Macrocyclization

The high diastereospecificity in the macrocyclization reaction of (S_P,S_P)-**7** with (*l*)-cyclohexane-1,2-diamine resembles the situation with the ethane-1,2-diyl-bridged analogue, where the selectivity was explained by conformational analysis of the N_2P_2 macrocycle based on X-ray data.[7e] The diastereospecificity is thus explained by conformational analysis of the intermediate in which the first of the two imine bonds has already formed (Chart 3). This intermediate preferably adopts a conformation in which the allylic 1,3-strain between the imine C-H bond and the tertiary carbon atom of the diamine backbone is minimized. Also, the lone pairs of the adjacent P and N donors point in opposite directions to minimize electronic (and steric) repulsion. With these restrictions, it is apparent that the intermediate is stereochemically prepared for the second condensation step only in the case of the (S_P,S_P)/(S_C,S_C)-diastereoisomer. In the (S_P,S_P)/(R_C,R_C)-intermediate, the amine and the formyl group point in opposite directions, which explains the formation of oligomers for this combination.

Bis(acetonitrile) Complex [Fe(MeCN)$_2$(1b)](BF$_4$)$_2$ (8b). The addition of an acetonitrile solution of [Fe(OH$_2$)$_6$](BF$_4$)$_2$ to the (NH)$_2$P$_2$ macrocycle (S_P,S_P,S_C,S_C)-**1b** in CH$_2$Cl$_2$/MeCN at 55 °C led to an immediate color change from light yellow to dark red (Scheme 4). The ^{31}P{^{1}H} NMR spectrum of the reaction mixture shows the presence of three different isomers in a 0.10:0.73:0.17 ratio. A singlet at δ 58.4 is assigned to the *trans* isomer *trans*-**8b**, whereas two AX systems are attributed to the two *cis*-β complexes *cis*-β-**8b** (δ 49.8 and 57.0, $^2J_{P,P'}$ = 60.5 Hz) and *cis*-β'-**8b** (δ 41.6 and 58.9, $^2J_{P,P'}$ = 62.5 Hz). As for the ethane-1,2-diyl derivative **8a** bearing macrocycle (S_P,S_P,S_C,S_C)-**1a**,[7b] the addition of DBU to this initial mixture led to complete isomerization to the thermodynamic product *cis*-β-**8b**, which was crystallized as a single isomer in 56% yield on a 1.46 g scale.

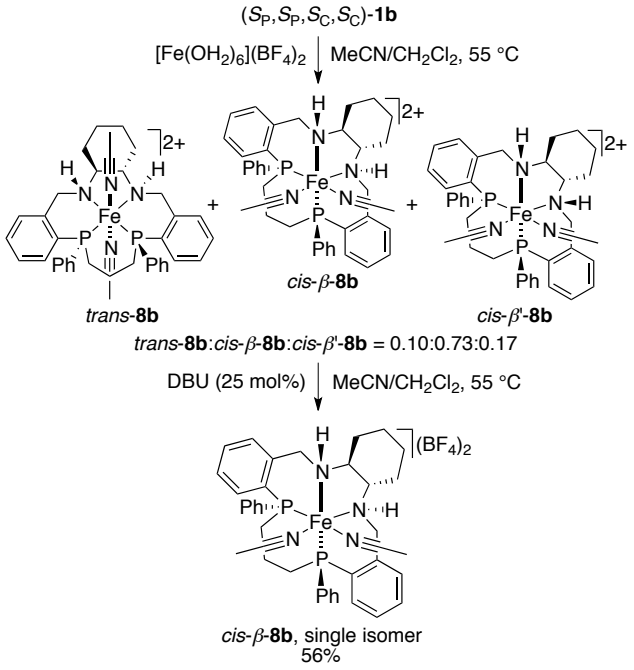

Scheme 4. Synthesis of Bis(acetonitrile) Complex 8b

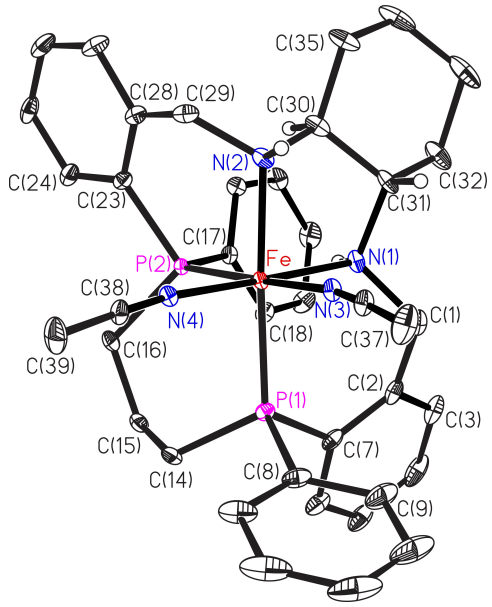

Figure 1. ORTEP drawing of the complex cation of *cis*-β-**8b** (ellipsoids at 30% probability).

An X-ray study of *cis*-β-**8b**, crystallized from MeCN/Et_2O, confirmed the assignment by $^{31}P\{^1H\}$ NMR spectroscopy (Figure 1). Despite the different ring size of the macrocyclic ligand, the structure of the new P–$(CH_2)_3$–P-linked bis(acetonitrile) complex [Fe(MeCN)$_2$((S_P,S_P,S_C,S_C)-**1b**)](BF$_4$)$_2$ (**8b**) is closely reminiscent of the ethane-1,2-diyl analogue [Fe(MeCN)$_2$((S_P,S_P,S_C,S_C)-**1a**)](BF$_4$)$_2$ (**8a**).[7e] As in **8a**, both nitrogen stereocenters in **8b** have the R_N absolute configuration, and the diamine unit adopts the characteristic stepped conformation. However, the change of the P–Fe–P chelate ring size causes subtle differences. Not surprisingly, the propane-1,3-diyl-bridged bis(acetonitrile) complex **8b** features significantly longer Fe–N and particularly Fe–P bond distances, as well as a larger P–P bite angle as compared to the ethane-1,2-diyl analogue **8a** (Table 1, omitted bond angles differ by less than 2° in **8a** and **8b**). The smaller P(1)–Fe–N(3) angle in **8b** involving one MeCN ligand is a symptom of enhanced steric crowding with the larger macrocycle **1b**.

Table 1. Selected Bond Lengths (Å) and Angles (°) in 8a and 8b

	cis-β-**8a**[7e]	*cis*-β-**8b**
Fe–P(1)	2.1837(7)	2.2187(12)
Fe–P(2)	2.1724 (6)	2.2193(11)
Fe–N(1)	2.020(2)	2.035(3)
Fe–N(2)	2.039(2)	2.048(4)
Fe–N(3)	1.962(2)	1.979(3)
Fe–N(4)	1.927(2)	1.932(3)
P(1)–Fe–P(2)	85.32(2)	92.92(4)
P(1)–Fe–N(1)	94.93(6)	94.32(11)
P(1)–Fe–N(2)	178.38(6)	176.16(11)
P(2)–Fe–N(1)	94.36(7)	93.25(11)
P(2)–Fe–N(2)	93.06(6)	90.75(11)
N(1)–Fe–N(2)	85.26(8)	84.35(15)
P(1)–Fe–N(3)	93.47(6)	89.39(11)

In contrast to bis(acetonitrile) complex **8a**, where the five-membered P(1)–Fe–P(2) chelate ring adopts a flexible half-chair conformation (Figure 2, left),[7e] the six-membered P(1)–Fe–P(2) chelate ring in the propane-1,3-diyl-linked analogue **8b** is in a chair conformation (Figure 2, right and Table S3). The rigid chair conformation is held in place by the diamine unit, which directs the benzylene linker between P(2) and N(2) to a *pseudo*-equatorial position and the benzylene linker between P(1) and N(1) to a *pseudo*-axial position of the six-membered chelate ring. A ring flip to the other chair conformation seems only possible with concomitant inversion of the N(2) stereocenter. Also, twist-boat or boat conformations are strongly disfavored due to strong steric repulsion with the ancillary acetonitrile ligand containing N(4) (not shown in Figure 2).

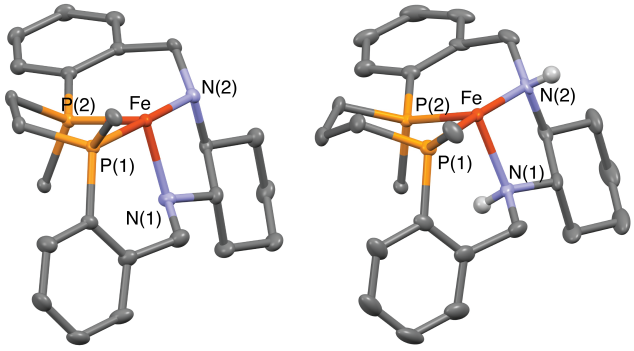

Figure 2. Comparison of the macrocyclic ligands (S_P,S_P,S_C,S_C)-**1a** in *cis*-β-**8a** (left)[7e] and (S_P,S_P,S_C,S_C)-**1b** in *cis*-β-**8b** (right). Phenyl substituents and hydrogen atoms are omitted for clarity.

The iron(II) bis(acetonitrile) complexes are a convenient entry point to the coordination chemistry of macrocyclic $(NH)_2P_2$ ligands.[7a] In view of our previous work[7] and the results reported by Morris,[3] we focused on the preparation of the bis(isonitrile) complexes [Fe(CNR)$_2$-((S_P,S_P,S_C,S_C)-**1b**)]$(BF_4)_2$ (**3**) and of the bromocarbonyl species [FeBr(CO)((S_P,S_P,S_C,S_C)-**1b**)]BPh_4 (**9**).

Bis(isonitrile) Complexes [Fe(CNR)$_2$(1b)](BF$_4$)$_2$ (3a-3c). The bis(acetonitrile) complex **8b** undergoes quantitative substitution of the ancillary acetonitrile ligands by $CNCEt_3$ and CN^iPr_2 within 24 h at 50 °C (Scheme 5). The corresponding bis(isonitrile) derivatives [Fe(CNR)$_2$-((S_P,S_P,S_C,S_C)-**1b**)]$(BF_4)_2$ (R = CEt_3, **3a**; N^iPr_2, **3b**) were obtained as a single configurational isomer in high yield. The *C*-isonitrile $CNCEt_3$ and the *N*-isonitrile CN^iPr_2 were the isonitriles of choice as the use of these sterically demanding isonitriles has previously been shown to lead to a vast increase in enantioselectivity for the ethane-1,2-diyl-bridged analogues **2** (*vide supra*).[7b]

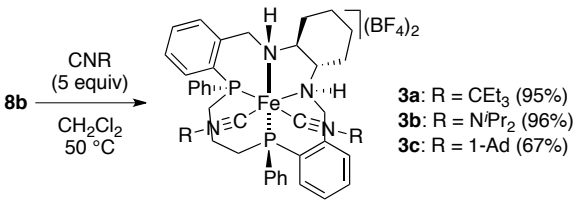

Scheme 5. Synthesis of Bis(isonitrile) Complexes 3a-3c

As iron(II) bis(1-adamantyl isonitrile) $(NH)_2P_2$ complexes are highly crystalline,[7b] the corresponding derivative **3c** (R = 1-Ad) was also prepared in order to gain structural information by X-ray diffraction. Crystals of the bis(1-adamantyl isonitrile) complex **3c** suitable for X-ray analysis were obtained from CH_2Cl_2/hexane. In the crystal structure, the macrocyclic ligand (S_P,S_P,S_C,S_C)-**1b** adopts a *cis*-β structure, with the two ancillary isonitriles completing the octahedral coordination sphere (Figure 3). The overall structure is closely related to the one of the bis(acetonitrile) complex **8b** (Table 2). As expected, the Fe–N(1) and Fe–P(2) distances in **3c** *trans* to the strong-field isonitrile ligands are slightly longer as compared to the bis(acetonitrile) complex **8b** due to the strong *trans* influence exerted by isonitriles.[7f]

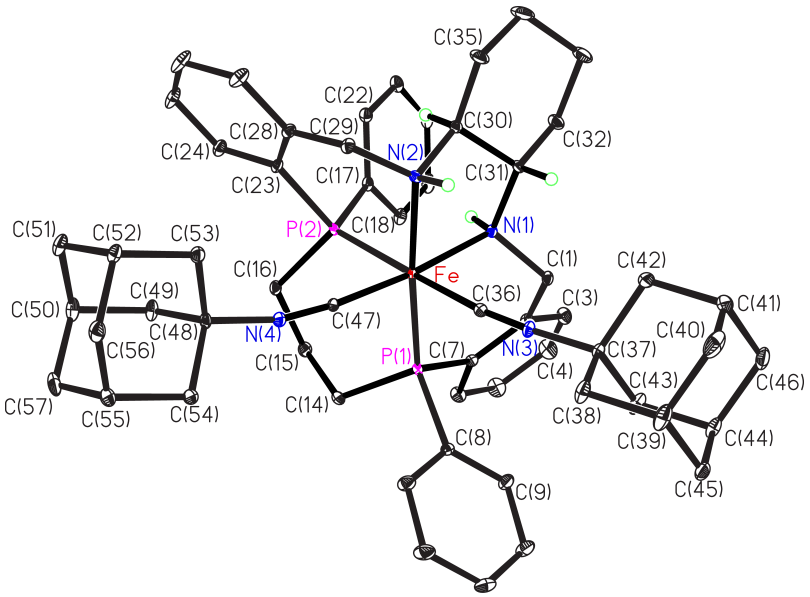

Figure 3. ORTEP drawing of the complex cation of *cis*-β-**3c** (ellipsoids at 30% probability).

Table 2. Selected Bond Lengths (Å) and (Torsion) Angles (°) in 3c and 8b

	cis-β-**3c**	*cis*-β-**8b**
Fe–P(1)	2.2174(7)	2.2187(12)
Fe–P(2)	2.2525(6)	2.2193(11)
Fe–N(1)	2.063(2)	2.035(3)
Fe–N(2)	2.072(2)	2.048(4)
Fe–C(36)	1.898(2)	–
Fe–C(47)	1.853(2)	–
P(1)–Fe–P(2)	92.42(2)	92.92(4)
P(1)–Fe–N(1)	92.14(6)	94.32(11)
P(1)–Fe–N(2)	174.71(6)	176.16(11)
P(1)–Fe–C(36)/N(3)	90.13(7)	89.39(11)
P(1)–Fe–C(47)/N(4)	92.56(7)	87.87(11)
P(2)–Fe–N(1)	92.94(6)	93.25(11)
P(2)–Fe–N(2)	89.44(6)	90.75(11)
P(2)–Fe–C(36)/N(3)	177.32(7)	175.81(11)
P(2)–Fe–C(47)/N(4)	84.34(7)	91.17(11)
N(1)–Fe–N(2)	82.82(8)	84.35(15)
N(1)–Fe–C(36)/N(3)	87.75(9)	90.06(14)
N(1)–Fe–C(47)/N(4)	174.66(9)	174.95(15)
N(2)–Fe–C(36)/N(3)	88.08(9)	87.01(15)
N(2)–Fe–C(47)/N(4)	92.55(9)	93.17(15)
C(36)/N(3)–Fe–C(47)/N(4)	94.76(10)	85.42(14)
C(1)–C(2)–C(7)–P(1)	–0.9(3)	9.4(6)
C(23)–C(28)–C(29)–N(2)	28.5(4)	43.3(6)
C(14)–P(1)–C(8)–C(9)	116.1(2)	145.1(4)

The macrocyclic $(NH)_2P_2$ ligand (S_P,S_P,S_C,S_C)-**1b** assumes very similar conformations in the bis(acetonitrile) complex **8b** and in the bis(isonitrile) complex **3c**. In particular, the angles and torsion angles in the six-membered P–Fe–P chelate ring in **8b** and **3c** differ by less than 2°. Only three torsion angles deviate more than 10° in the two complexes, and the largest difference affects the C(14)–P(1)–C(8)–C(9) angle, resulting from different orientations of the phenyl substituent on P(1). In **3c**, the phenyl group rotates by ca. 30° to accommodate the larger adamantyl substituent. Thus, the propane-1,3-diyl-linked macrocycle (S_P,S_P,S_C,S_C)-**1b** is more rigid than its $(CH_2)_2$ analogue (S_P,S_P,S_C,S_C)-**1a**, in which the five-membered P–Fe–P chelate is flexible and can adopt different half-chair conformations as shown previously.[7b] Furthermore, the bond angles involving the macrocycle are very similar in **3c** and **8b**, whereas those involving the ancillary ligands (MeCN and CNAd) vary widely. This further suggests that macrocycle **1b** forms a rigid coordination pocket (Table 2).

Bromocarbonyl Complex [FeBr(CO)(1b)]BPh_4 (9). Besides bis(isonitrile) complexes **3**, we targeted the bromocarbonyl complex [FeBr(CO)((S_P,S_P,S_C,S_C)-**1b**)]BPh_4 (**9**), as related iron(II)/P(NH)NP complexes are highly active ATH catalysts and achieve TOFs up to 200 s^{-1} (see Chart 1).[3] In analogy to Morris' system, the bromocarbonyl complex **9** was prepared from the bis(acetonitrile) complex **8b** and KBr (2 equiv) in acetone under a CO atmosphere. The reaction afforded a single new species as indicated by $^{31}P\{^1H\}$ NMR spectroscopy (δ 21.3 and 39.0, $^2J_{P,P'}$ = 69.6 Hz), which was isolated as the tetraphenylborate salt [FeBr(CO)(S_P,S_P,S_C,S_C)-**1b**)]BPh_4 (**9**) (Scheme 6).

The large difference in the $^2J_{P,C}$ coupling of the phosphines to CO in the $^{13}C\{^1H\}$ NMR spectrum (δ 216.0 (dd, $^2J_{P,C}$ = 52.7, 25.4 Hz) suggests a *cis-β* isomer with CO *trans* to phosphorus and bromide *trans* to amine, as previously observed for related species.[7e] For the other *cis-β*

isomer with CO *trans* to amine and bromide *trans* to phosphorus (and also for *trans* isomers), similar $^{2}J_{P,C}$ coupling constants are expected as both phosphines are *cis* to CO (and not one *trans* and one *cis* as in **9**). Unfortunately, as all attempts to obtain suitable crystals failed, this assignment is not confirmed by X-ray crystallography.

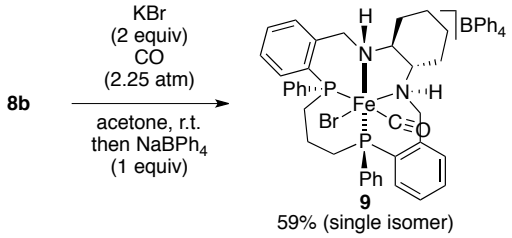

Scheme 6. Synthesis of Bromocarbonyl Complex 9

Asymmetric Transfer Hydrogenation. The newly prepared complexes containing the propane-1,3-diyl-bridged macrocycle **1b**, that is, the bis(acetonitrile) derivative **8b**, the bis(isonitrile) analogue **3a**-**3c** (R = CEt_3, **3a**; N^iPr_2, **3b**; 1-Ad, **3c**), and the bromocarbonyl complex **9**, were tested as catalysts in the ATH of acetophenone (**10a**) as standard substrate (Table 3). The ATH reactions were performed in the presence of NaO^tBu (S/C/B = 400/1/10) in ^{i}PrOH (0.2 M in substrate) at 40 °C, and the reactions were followed by GC. For the sake of comparison, **10a** was hydrogenated under these conditions with the previously reported ethane-1,2-diyl bis(isonitrile) catalysts $[Fe(CNR)_2((S_P,S_P,S_C,S_C)$-**1a**$)](BF_4)_2$ (R = CEt_3, **2a**; R = N^iPr_2, **2b**).[7b]

The screening showed that the bis(acetonitrile) complex **8b** achieves only 1% conversion to 1-phenylethan-1-ol after 1 h (entry 1) and is hence essentially inactive as ATH catalyst. This is in line with previous results showing that Fe(II) bis(acetonitrile) complexes are poor catalysts,[7d] possibly because acetonitrile does not efficiently stabilize low-valent iron(II) intermediates. The catalyst activity increases on going from bis(acetonitrile) (**8b**) to bromocarbonyl (**9**) and even

more to the bis(isonitrile) motive (**3a**). This suggests that π-accepting ligands increase the catalyst activity, but is in contrast with Morris' finding that the bromocarbonyl complexes are the most active iron-based ATH catalysts.[3k]

The enantioselectivity increases along with the steric bulk of the ancillary ligands from bromocarbonyl **9** (86% ee, 5 min, entry 2) to **3a** (R = CEt_3, 98% ee, 5 min, entry 3) and **3b** (R = N^iPr_2, 99% ee, 1 h, entry 4). However, the activity of the latter is considerably lower than that of the less bulky $CNCEt_3$ analogue **3a**. Accordingly, the bis(1-adamantyl isonitrile) complex **3c** is the most active catalyst (average TOF was 3 700 h^{-1} after 5 min). However, it gives only 92% ee after 5 min (entry 5), and the enantioselectivity declines during the reaction (81% ee after 1 h) as the equilibrium position is approached. Therefore, catalysts **3a** and **3b** were chosen for the screening of the substrate scope (see below).

Table 3. Catalyst Screening in the ATH of Acetophenone (10a)[a]

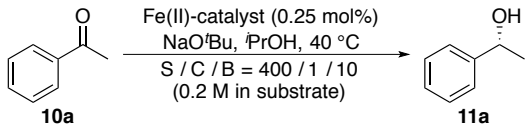

entry	catalyst	after 5 min		after 60 min	
1	**8b**	<1%	–	1%	–
2	**9**	14%	86% ee	77%	84% ee
3	**3a** (R = CEt_3)	50%	98% ee	92%	98% ee
4	**3b** (R = N^iPr_2)	4%	–	33%	99% ee
5	**3c** (R = 1-Ad)	78%	92% ee	93%	81% ee
6	**2a** (R = CEt_3)	17%	97% ee	91%	96% ee
7	**2b** (R = N^iPr_2)	8%	98% ee	47%	98% ee

[a] Reactions were performed on a 1.0 mmol scale in ^{i}PrOH (0.2 M in substrate). Conversions and ee values were determined by GC.

Compared with their ethane-1,2-diyl analogues **2a** and **2b**, the propane-1,3-diyl-bridged catalysts **3a** and **3b** reduce acetophenone with higher enantioselectivity under identical reaction conditions (98 and 99% ee vs. 96 and 98% ee, respectively) (entries 3, 4, 6, and 7). Interestingly, the propane-1,3-diyl-based *C*-isonitrile complex **3a** is also more active than **2a** and **2b**, which shows that the increased macrocycle size and hence enhanced steric crowding at the metal are not necessarily detrimental to activity.

Before investigating the substrate scope, the reactions conditions with catalysts **3a** and **3b** were further optimized. Catalyst loadings of 0.1 and 0.02 mol% (instead of 0.25 mol%) left the enantioselectivity of acetophenone reduction unchanged, even though higher reaction temperatures and longer times were used to achieve high conversions (Table 4). This emphasizes the robustness of the macrocyclic iron(II)/$(NH)_2P_2$ catalyst system and is in line with the successful scale-up studies performed for the ethane-1,2-diyl-bridged analogues **2a** and **2b**.[7c]

Table 4. Effect of Catalyst Loading on the ATH of Acetophenone (10a)[a]

entry	catalyst (mol%)	**10a** (mmol)	S / C / B	*T* (°C)	*t* (h)	conv. (%)	ee (%)
1	**3a** (0.25)	1.0	400/1/10	40	1.0	92	98
2	**3a** (0.1)	2.5	1 000/1/10	50	0.5	93	98
3	**3a** (0.02)	5.0	5 000/1/20	60	1.5	91	98
4	**3b** (0.25)	1.0	400/1/10	40	1.0	33	99
5	**3b** (0.1)	2.5	1 000/1/10	60	1.5	93	99
6	**3b** (0.02)	5.0	5 000/1/20	75	1.5	93	99

[a] Reaction solutions were 0.2 M in substrates, NaO^{t}Bu was used as base, conversions and ee values were determined by GC.

Substrate Scope. A broad set of substrates bearing polar double bonds (Chart 4) was reduced with the propane-1,3-diyl-linked catalysts **3a** and **3b** under the conditions of entries 2 and 5 in Table 4 (0.1 mol% of catalyst, 50 and 60 °C, respectively), which allows full comparison with catalysts **2a** and **2b** (see below and Chart S2).[7b]

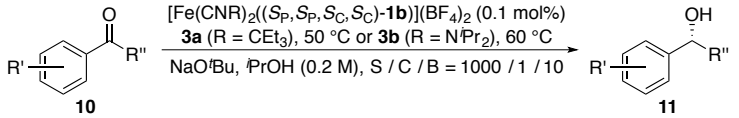

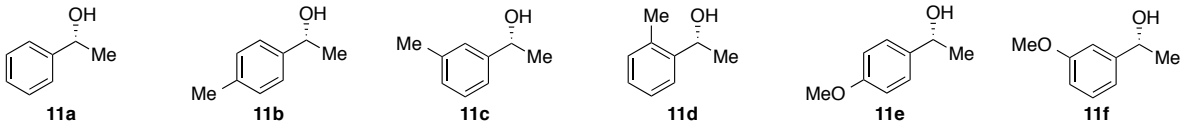

3a (0.5 h): 93%, 98% ee **3a** (0.5 h): 86%, 96% ee **3a** (0.5 h): 90%, 98% ee **3a** (5.0 h): 81%, 97% ee **3a** (0.5 h): 72%, 96% ee **3a** (0.5 h): 92%, 97% ee
3b (1.5 h): 91%, 99% ee **3b** (1.0 h): 87%, 98% ee **3b** (1.5 h): 91%, 98% ee **3b** (5.0 h): 65%, 99% ee **3b** (1.5 h): 71%, 97% ee **3b** (1.0 h): 92%, 98% ee

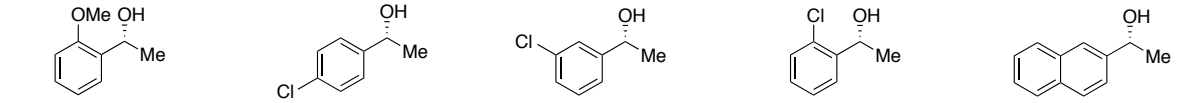

3a (5.0 h): 82%, 98% ee **3a** (0.5 h): 97%, 96% ee **3a** (0.25 h): 97%, 97% ee **3a** (5.0 h): 97%, 97% ee **3a** (0.5 h): 93%, 93% ee
3b (5.0 h): 44%, 92% ee **3b** (1.0 h): 97%, 97% ee **3b** (1.0 h): 98%, 97% ee **3b** (5.0 h): 77%, 97% ee **3b** (1.0 h): 92%, 98% ee

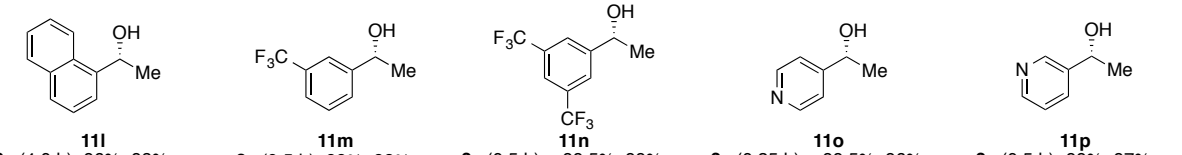

3a (4.0 h): 96%, 98% ee **3a** (0.5 h): 99%, 98% ee **3a** (0.5 h): >99.5%, 99% ee **3a** (0.25 h): >99.5%, 96% ee **3a** (0.5 h): 99%, 97% ee
3b (5.0 h): 90%, 99% ee **3b** (2.0 h): 99%, 98% ee **3b** (5.0 h): 61%, 84% ee **3b** (5.0 h): 60%, 95% ee **3b** (2.0 h): 99%, 93% ee

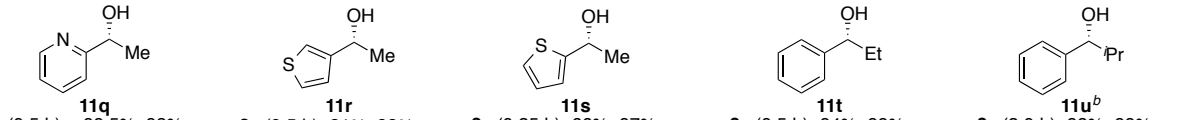

3a (0.5 h): >99.5%, 98% ee **3a** (0.5 h): 81%, 98% ee **3a** (0.25 h): 66%, 97% ee **3a** (0.5 h): 94%, 99% ee **3a** (3.0 h): 98%, 99% ee
3b (1.5 h): 99%, 87% ee **3b** (1.0 h): 83%, 97% ee **3b** (1.0 h): 71%, 96% ee **3b** (1.5 h): 94%, 99% ee **3b** (1.5 h): 98%, 99% ee

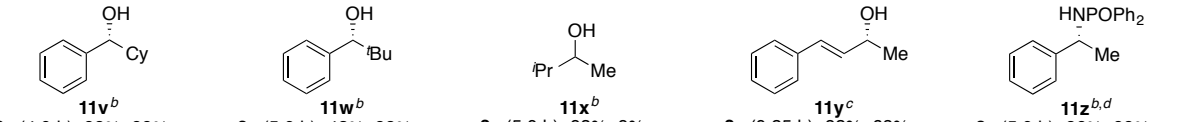

3a (4.0 h): 98%, 99% ee **3a** (5.0 h): 42%, 98% ee **3a** (5.0 h): 93%, 9% ee **3a** (0.25 h): 82%, 68% ee **3a** (5.0 h): 86%, 99% ee
3b (1.0 h): 97%, >99.5% ee **3b** (5.0 h): 65%, 99% ee **3b** (2.5 h): 98%, 5% ee **3b** (1.0 h): 81%, 69% ee **3b** (5.0 h): 81%, 79% ee

[a] Reactions were performed on a 2.5 mmol scale in [i]PrOH (0.2 M). Conversion and enantiomeric excess were determined by GC or HPLC. [b] Reaction performed on a 0.625 mmol scale with S/C/B = 250/1/10 at 75 °C. [c] Complete chemoselectivity for the allylic alcohol observed (saturated products <1%). [d] Isolated yield.

Chart 4. ATH of Substrates Containing Polar Double Bonds with Catalysts 3a and 3b[a]

The reactions with chloro-, methyl-, or methoxy-substituted aryl methyl ketones (**10b**-**10j**) and with acetonaphthones (**10k** and **10l**) showed that *para*- and *meta*-substitution is well tolerated. The corresponding optically active alcohols were obtained with excellent enantioselectivity (93–98% ee, ≥97% ee for the more selective catalyst) within 0.5–1.5 h (TOF = 470 to 3 890 h^{-1}). In stark contrast, the hydrogenation of *ortho*-substituted substrates **10d**, **10g**, **10j**, and **10l** was still highly enantioselective (92–99% ee, ≥97% ee for the more selective catalyst), but the reactions were much slower and only moderate conversions (44–97%) were obtained after 4.0–5.0 h (TOF = 90 to 240 h^{-1}). A similar trend has been observed with the P–$(CH_2)_2$–P-based complexes **2a** and **2b**,[7b] but catalysts **3a** and **3b** are much more sensitive to steric effects as discussed below. Overall, electronic effects were less pronounced for catalysts **3**, and both electron-rich and electron-poor ketones were reduced with excellent enantioselectivity.

The industrially relevant trifluoromethylated ketones **10m** and **10n** were rapidly hydrogenated by the $CNCEt_3$ derivative **3a**. The corresponding alcohols **11m** and **11n**, which are important building blocks for fungicides[10] and NK_1 antagonists,[9] were obtained in quantitative yield within 0.5 h and with 98% and 99% ee, respectively. In both cases, average TOFs of >1 950 h^{-1} were measured. The results differ strongly from the ones obtained with *N*-isonitrile catalyst **3b**, which only performed poorly with these substrates, and show again the pivotal role played by the tuning of the isonitrile ligand.

Complex **3a** was also the catalyst of choice for the ATH of acyl-substituted heterocycles (**10o**-**10s**). Acyl pyridines **10o**-**10q** were reduced in quantitative yield and with 96–98% ee within 0.25–0.5 h with no sign of catalyst poisoning by the pyridine substrate. The highest activity was achieved in the case of 4-acetylpyridine (**10o**), for which the average TOF was >3 950 h^{-1}. Acyl thiophenes **10r** and **10s** were also reduced by **3a** within 0.25–0.5 h with 98 and 97% ee,

respectively, but the conversions were significantly lower than for acyl pyridines (83 and 71% for acyl thiophenes **10r** and **10s**, respectively). The electron-rich thiophene moiety, which shifts the ATH equilibrium toward the ketone, probably account for the low conversions, rather than catalyst decomposition or poisoning by the thiophene group. Again, the *N*-isonitrile catalyst **3b** was inferior to *C*-isonitrile catalyst **3a** for these acyl heterocycles.

Phenyl alkyl ketones bearing larger alkyl groups (**10t**-**10w**) were also tested. Catalyst **3a** was superior in the reduction of propiophenone (**10t**) to (*R*)-1-phenylpropan-1-ol (94% conversion, 99% ee after 0.5 h), whereas the *N*-isonitrile catalyst **3b** gave better results for substrates bearing secondary and tertiary alkyl groups (**10u**-**10w**). The catalyst loading (0.4 mol%) and reaction temperature (75 °C) were slightly increased with these substrates to ensure rapid conversion to the optically active alcohols. Under these optimized conditions, *iso*-propyl phenyl ketone (**10u**) and cyclohexyl phenyl ketone (**10v**) were reduced by *N*-isonitrile catalyst **3b** in 98% yield and with outstanding ≥99% ee within 1.0–1.5 h.

The enantioselectivity was also high in the case of *tert*-butyl phenyl ketone (**10w**, 99% ee), but the reaction was sluggish and only 65% conversion was achieved after 5.0 h. Again, this finding shows that the propane-1,3-diyl-bridged complexes **3a** and **3b** are rather sensitive toward sterically demanding substrates.

A dialkyl ketone such as **10x** was reduced with poor enantioselectivity with either catalyst (9% and 5% ee for **3a** and **3b** respectively). Thus, similarly to their $(CH_2)_2$-linked analogues **2**,[7b] the bis(isonitrile) catalysts **3** readily differentiate between an aromatic and an aliphatic substituent, but not between two alkyl substituents of different size. On these lines, enone **10y** was reduced with modest enantioselectivity (68% and 69% for **3a** and **3b**, respectively), which further

indicates that an aryl group conjugated with the polar double bond is essential for good enantiodiscrimination.

Finally, the *C*-isonitrile catalyst **3a** efficiently hydrogenates the phosphinyl imine **10z**, and the reduced product **11z** was isolated in 86% yield and with 99% ee after flash column chromatography. Phosphinyl imines are efficient precursors to enantiopure primary amines as the phosphinyl group in **11z** is readily cleaved by ethanolic hydrochloric acid without loss of configuration at the adjacent stereocenter.[15]

Substrate Scope: Discussion. A previous comparison with state-of-the-art iron-based catalysts[7c] has shown that the ethane-1,2-diyl analogues **2a** and **2b** and Gao's system[4] (see Chart 1) are the only ones that combine high activity with excellent enantioselectivity for a broad scope of substrates. However, rational modification of the latter catalyst is difficult, as it is prepared *in situ* and is poorly defined. Also, poisoning experiments and the observation of a long activation period suggest the involvement of iron nanoparticles. Morris' 3rd generation P(NH)NP catalysts are the most active in the series, but their enantioselectivity exceeds 95% ee only with a few substrates (**10a**, **10n** and α-chloroacetophenone).[3k,m] Therefore, the propane-1,3-diyl-bridged complexes **3a** and **3b** are benchmarked here with the ethane-1,2-diyl analogues **2a** and **2b** (for a full comparison see Chart S2).

The propane-1,3-diyl-linked complexes **3a** and **3b** hydrogenate *meta*- and *para*-substituted acetophenones (**10b**, **10c**, **10d**, **10e**, **10f**, **10h**, **10i**, **10k**, and **10m**) to the corresponding alcohols with higher activity and enantioselectivity than their $(CH_2)_2$-bridged analogues **2a** and **2b**. Overall, **3a** and **3b** achieve 93–98% ee (≥97% ee for the more selective catalyst), while catalysts **2** give 91–98% ee (≥94% ee for the more selective catalyst).[7b] The differences seem negligible in percentage, but the absolute increase in $\Delta\Delta G^{\ddagger}$ is considerable, also taking into account that **2** and

3 differ only for a single methylene unit in the macrocyclic ligand. However, the ethane-1,2-diyl-bridged catalysts **2a** and **2b** are significantly more active than **3a** and **3b** in the hydrogenation of the sterically demanding, *ortho*-substituted acetophenones (**10d**, **10g**, **10j**, and **10l**).

We tentatively invoke steric and conformational effects of the macrocyclic ligand to explain the higher enantioselectivity and increased sensitivity to steric effects of catalysts **3** as compared to **2**. In fact, the larger P–Fe–P bite angle (and possibly the longer Fe–ligand bonds) of **1b** as compared to **1a** increases the steric bulk of the macrocycle, and the decreased flexibility of the P–Fe–P chelate ring in the $(CH_2)_3$-linked catalysts **3** reinforces this effect by preventing the P–Fe–P chelate to move out of the trajectory of the incoming acetophenone. Overall, this leads to increased enantioselectivity, but also to increased activation energy with sterically demanding substrates.

The above hypothesis is corroborated by the results obtained for phenyl alkyl ketones **10t**-**10w**, which are reduced with higher enantioselectivity (98–99.6% ee) by the propane-1,3-diyl-linked complexes **3a** and **3b** than by the $(CH_2)_2$ analogues **2** (86–98% ee). Phenyl alkyl ketones with primary or secondary alkyl groups are hydrogenated rapidly, but a strong decrease in activity is observed for *tert*-butyl phenyl ketone (**10w**, 65% conversion after 5 h with catalyst **3b**). However, **10w** is efficiently reduced to the corresponding secondary alcohol (*R*)-**11w** in quantitative yield and with 97% ee within 4.0 h by the $(CH_2)_2$ analogue **2b**.[7b]

For the acyl heterocycles **10o**-**10s**, the propane-1,3-diyl-based *C*-isonitrile complex **3a** is the catalyst of choice and achieves 96–98% ee (vs. 92–98% ee for the better performing of the ethane-1,2-diyl analogues **2a** and **2b**). Furthermore, **3a** was by far the most active catalyst for all heterocyclic substrates (the TOF was up to >3 950 h^{-1} for **10o**). With most substrates, changing from *C*-isonitrile $CNCEt_3$ to *N*-isonitrile CNN^iPr_2 affects the enantioselectivity marginally

(usually within 5%). However, the *C*-isonitrile complex **3a** hydrogenates 2-acetylpyridine (**10q**) with impressive 98% ee, whereas the *N*-isonitrile derivative **3b** gives only 87% ee. A similar difference was also observed for 3,5-bis(trifluoromethyl)acetophenone (**10n**, 99% and 84% ee for **3a** and **3b**, respectively) and for the phosphinyl imine **10z** (99% and 79% ee for **3a** and **3b**, respectively), but its origin is currently unclear.

In summary, complexes **2** and **3** are complementary to a certain extent. The propane-1,3-diyl-bridged complexes **3a** and **3b** efficiently reduce sterically less demanding substrates such as *para*- and *meta*-substituted aryl alkyl ketones, acyl heterocycles, and aryl alkyl ketones with primary or secondary alkyl groups. High enantioselectivity (≥96% ee) is obtained with the more selective catalyst. Sterically more demanding substrates that are hydrogenated by **3** with low activity are efficiently reduced by the ethane-1,2-diyl analogues **2a** and **2b** (≥97% ee for the more selective catalyst), which are less sensitive to steric bulk.[7b] In the light of these considerations, the importance of catalyst modularity is obvious.

Complex Design. In this section, we highlight the possible sites for catalyst tuning and optimization for the iron(II)/$(NH)_2P_2$ bis(isonitrile) complexes. As shown above, the strategy based on Han's *H*-phosphinate (R_P)-**4** allows to easily change from an ethane-1,2-diyl to a propane-1,3-diyl bridge (Chart 5, blue). However, this modification is not necessarily restricted to a three-carbon bridge, as different backbones, e.g. longer ones, seem feasible.

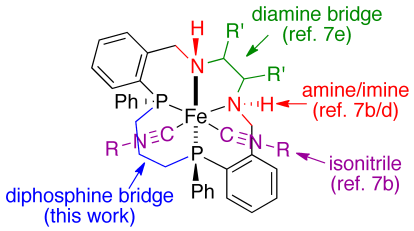

Chart 5. Possible Catalyst Modifications

We have shown previously that the diamine can be changed from (1*S*,2*S*)-diaminocyclohexane1-2-diamine to (1*R*,2*R*)-diphenylethane-1,2-diamine in the *matched* macrocyclization step (Chart 5, green).[7e] Furthermore, the diimino macrocycles[7d] can be reduced to the diamino analogues,[7b] whose complexes are three orders of magnitude more active as ATH catalysts (Chart 5, red). Finally, the R group of the CNR isonitrile ligands, which are introduced in the last step of the catalyst preparation, can be widely varied, as a plethora of isonitriles are commercially available or can be prepared in few steps (Chart 5, violet).[7b-d] The present and previous[7b,c] examples underscore the success of this strategy and show that, with these handles, the macrocyclic iron(II)/$(NH)_2P_2$ catalysts build a flexible platform that allows facile optimization for individual substrates.

So far, we have explored the effect of tuning the CNR ligands,[7b,c] of changing imine to amine,[7b,d] and of adding a methylene group to the bridge between the phosphines (this paper), but further sites of the catalysts can be addressed. Thus, our group is currently exploring the effect of changing the aryl substituents on the phosphorus donors (i.e. the exo-aryl substituent and the benzylene linker to nitrogen) extending the protocol described herein to different *H*-phosphinates.[14] To get insight into the catalytically active species and develop a stereochemical model for the reaction, we are also preparing hydride complexes with the $(NH)_2P_2$ macrocycles, but their formulation and stereochemistry are still under investigation.

CONCLUSION AND OUTLOOK

In this work, we have presented the synthesis of the propane-1,3-diyl-bridged $(NH)_2P_2$ macrocycle (S_P,S_P,S_C,S_C)-**1b** in 6 steps and high yield from Han's *H*-phosphinate (R_P)-**4**. As (S_P)-**4** is also available by using (+)- instead of (–)-menthol, both enantiomers of the macrocycle (and, consequently, of the iron(II) catalysts) are accessible, ultimately guaranteeing access to both

enantiomers of the catalysis products. The new protocol based on menthol[7c] guarantees the availability of the $(NH)_2P_2$ macrocycles on a multigram scale, as well as the tuning of the diphosphine bridge.

The addition of a single methylene unit into the macrocycle strongly affects the outcome of catalysis, as catalysts of type **3** are significantly more active and enantioselective with most substrates than their previously reported ethane-1,2-diyl analogues **2**. Thus, this study shows that minute, facile changes in catalyst design alter the catalyst performance considerably, which can be rationalized by careful analysis of X-ray structural data. This opens the way to effective individual optimization of each substrate, also in combination with the tuning of the isonitrile ligand, as demonstrated in this paper and before.[7b,c] Therefore, the present class of macrocyclic iron(II) complexes truly constitutes a family of catalysts that can be easily prepared, structurally characterized, and systematically modified. These properties are the *sine qua non* for rational catalyst design, in combination with mechanistic understanding and a stereochemical model for enantioselection, which are among our next goals.

Independently from future developments, the propane-1,3-diyl-bridged catalysts **3a** and **3b** described herein, as well as the previously reported ethane-1,2-diyl-based analogues **2a** and **2b**, form a toolbox for the efficient and highly enantioselective transfer hydrogenation of aryl alkyl ketones and bring the development of cost-efficient base metals catalyst for such reactions closer at hand.

AUTHOR INFORMATION

Corresponding Author

* E-mail: mezzetti@inorg.chem.ethz.ch

Notes

The authors declare no competing financial interest.

ASSOCIATED CONTENT

Supporting Information Available: Detailed experimental procedures and characterization of all products (PDF), crystallographic information file for complexes **3c** and **8b** (CIF). This material is available free of charge via the Internet at http://pubs.acs.org.

ACKNOWLEDGMENT

We thank the Swiss National Science Foundation for financial support (grant no. 200020_146881).

REFERENCES

(1) (a) Blaser, H.-U.; Spindler, F.; Studer, M. *Appl. Catal. A.: General* **2001**, *221*, 119–143. (b) *Asymmetric Catalysis on Industrial Scale: Challenges, Approaches and Solutions*, 2nd ed.; Blaser, H.-U., Federsel, H.-J., Eds.; Wiley-VCH: Weinheim, 2010. (c) Busacca, C. A.; Fandrick, D. R.; Song, J. J.; Senanayake, C. H. *Adv. Synth. Catal.* **2011**, *353*, 1825–1864. (d) Blaser, H.-U.; Pugin, B.; Spindler, F. *Top. Organomet. Chem.* **2012**, *42*, 65–102. (e) Magano, J.; Dunetz, J. R. *Org. Process Res. Dev.* **2012**, *16*, 1156–1184. (f) Ager, D. J.; de Vries, A. H. M.; de Vries, J. G. *Chem. Soc. Rev.* **2012**, *41*, 3340–3380.

(2) For selected reviews, see: (a) Darcel, C.; Sortais, J.-B. *Top. Organomet. Chem.* **2015**, *50*, 173–216. (b) Misal Castro, L. C.; Li, H.; Sortais, J.-B.; Darcel, C. *Green Chem.* **2015**, *17*, 2283–2303. (c) Bauer, I.; Knölker, H.-J. *Chem. Rev.* **2015**, *115*, 3170–3387. (d) Nakazawa, H.; Itazaki,

M. *Top. Organomet. Chem.* **2011**, *33*, 27–81. (e) Le Bailly, B. A. F.; Thomas, S. P. *RSC Adv.* **2011**, *1*, 1435–1445.

(3) For selected articles, see: (a) Morris, R. H. *Acc. Chem. Res.* **2015**, *48*, 1494–1502. (b) Sues, P. E.; Demmans, K. Z.; Morris, R. H. *Dalton Trans.* **2014**, *43*, 7650–7667. (c) Sui-Seng, C.; Freutel, F.; Lough, A. J.; Morris, R. H. *Angew. Chem. Int. Ed.* **2008**, *47*, 940–943. (d) Sui-Seng, C.; Haque, F. N.; Hadzovic, A.; Pütz, A.-M.; Reuss, V.; Meyer, N.; Lough, A. J.; Zimmer-De Iuliis, M.; Morris, R. H. *Inorg. Chem.* **2009**, *48*, 735–743. (e) Sonnenberg, J. F.; Coombs, N.; Dube, P. A.; Morris, R. H. *J. Am. Chem. Soc.* **2012**, *134*, 5893–5899. (f) Mikhailine, A.; Lough, A. J.; Morris, R. H. *J. Am. Chem. Soc.* **2009**, *131*, 1394–1395. (g) Lagaditis, P. O.; Lough, A. J.; Morris, R. H. *J. Am. Chem. Soc.* **2011**, *133*, 9662–9665. (h) Sues, P. E.; Lough, A. J.; Morris, R. H. *Organometallics* **2011**, *30*, 4418–4431. (i) Mikhailine, A. A.; Maishan, M. I.; Morris, R. H. *Org. Lett.* **2012**, *14*, 4638–4641. (j) Mikhailine, A. A.; Maishan, M. I.; Lough, A. J.; Morris, R. H. *J. Am. Chem. Soc.* **2012**, *134*, 12266–12280. (k) Zuo, W.; Lough, A. J.; Li, Y. F.; Morris, R. H. *Science* **2013**, *342*, 1080–1083. (l) Zuo, W.; Tauer, S.; Prokopchuk, D. E.; Morris, R. H. *Organometallics* **2014**, *33*, 5791–5801. (m) Smith, S. A. M.; Morris, R. H. *Synthesis* **2015**, *47*, 1775–1779. (n) Zuo, W.; Prokopchuk, D. E.; Lough, A. J.; Morris, R. H. *ACS Catal.* **2016**, *6*, 301–314. (o) Lagaditis, P. O.; Sues, P. E.; Sonnenberg, J. F.; Wan, K. Y.; Lough, A. J.; Morris, R. H. *J. Am. Chem. Soc.* **2014**, *136*, 1367–1380.

(4) (a) Li, Y.-Y.; Yu, S.-L.; Shen, W.-Y.; Gao, J.-X. *Acc. Chem. Res.* **2015**, *48*, 2587–2598. (b) Chen, J.-S.; Chen, L.-L.; Xing, Y.; Chen, G.; Shen, W.-Y.; Dong, Z.-R.; Li, Y.-Y.; Gao, J.-X. *Acta Chim. Sin.* **2004**, *62*, 1745–1750. (c) Yu, S.; Shen, W.; Li, Y.; Dong, Z.; Xu, Y.; Li, Q.; Zhang, J.; Gao, J. *Adv. Synth. Catal.* **2012**, *354*, 818–822. (d) Li, Y.; Yu, S.; Wu, X.; Xiao, J.; Shen, W.; Dong, Z.; Gao, J. *J. Am. Chem. Soc.* **2014**, *136*, 4031–4039.

(5) (a) Bleith, T.; Wadepohl, H.; Gade, L. H. *J. Am. Chem. Soc.* **2015**, *137*, 2456–2459. (b) Bleith, T.; Gade, L. H. *J. Am. Chem. Soc.* **2016**, *138*, 4972–4983. (c) Langlotz, B. K.; Wadepohl, H.; Gade, L. H. *Angew. Chem. Int. Ed.* **2008**, *47*, 4670–4674.

(6) (a) Zhou, S.; Fleischer, S.; Junge, K.; Beller, M. *Angew. Chem. Int. Ed.* **2011**, *50*, 5120–5124. (b) Fleischer, S.; Zhou, S.; Werkmeister, S.; Junge, K.; Beller, M. *Chem. Eur. J.* **2013**, *19*, 4997–5003. (c) Lu, L.-Q.; Li, Y.; Junge, K.; Beller, M. *J. Am. Chem. Soc.* **2015**, *137*, 2763–2768.

(7) (a) Bigler, R.; Huber, R.; Mezzetti, A. *Synlett* **2016**, *27*, 831–847. (b) Bigler, R.; Huber, R.; Mezzetti, A. *Angew. Chem. Int. Ed.* **2015**, *54*, 5171–5174. (c) Bigler, R.; Mezzetti, A. *Org. Process Res. Dev.* **2016**, *20*, 253–261. (d) Bigler, R.; Mezzetti, A. *Org. Lett.* **2014**, *16*, 6460–6463. (e) Bigler, R.; Otth, E.; Mezzetti, A. *Organometallics* **2014**, *33*, 4086–4099. (f) Huber, R.; Bigler, R.; Mezzetti, A. *Organometallics* **2015**, *34*, 3374–3384.

(8) (a) Dong, Z.-R.; Li, Y.-Y.; Chen, J.-S.; Li, B.-Z.; Xing, Y.; Gao, J.-X. *Org. Lett.* **2005**, *7*, 1043–1045. (b) Clarke, M. L. *Synlett* **2014**, *25*, 1371–1380. (c) Noyori, R.; Ohkuma, T. *Angew. Chem. Int. Ed.* **2001**, *40*, 40–73. (d) Dong, Z.-R.; Li, Y.-Y.; Chen, J.-S.; Li, B.-Z.; Xing, Y.; Gao, J.-X. *Org. Lett.* **2005**, *7*, 1043–1045. (e) Ohkuma, T.; Sandoval, C. A.; Srinivasan, R.; Lin, Q.; Wei, Y.; Muñiz, K.; Noyori, R. *J. Am. Chem. Soc.* **2005**, *127*, 8288–8289. (f) Clarke, M. L.; Díaz-Valenzuela, M. B.; Slawin, A. M. Z. *Organometallics* **2007**, *26*, 16–19.

(9) Brands, K. M. J.; Payack, J. F.; Rosen, J. D.; Nelson, T. D.; Candelario, A.; Huffman, M. A.; Zhao, M. M.; Li, J.; Craig, B.; Song, Z. J.; Tschaen, D. M.; Hansen, K.; Devine, P. N.; Pye, P. J.; Rossen, K.; Dormer, P. G.; Reamer, R. A.; Welch, C. J.; Mathre, D. J.; Tsou, N. N.; McNamara, J. M.; Reider, P. J. *J. Am. Chem. Soc.* **2003**, *125*, 2129–2135.

(10) (a) Tanaka, K.; Katsurada, M.; Ohno, F.; Shiga, Y.; Oda, M.; Miyagi, M.; Takehara, J.; Okano, K. *J. Org. Chem.* **2000**, *65*, 432–437. (b) Miyagi, M.; Takehara, J.; Collet, S.; Okano, K. *Org. Process Res. Dev.* **2000**, *4*, 346–348.

(11) The $CNCPr_3$ and CNTMP derivatives gave similar results to the parent complexes **2a** and **2b**, whereas the synthesis of $CNCBn_3$, CNC^iPr_3, and $CNC(CH_2{}^tBu)_3$ failed, and elimination products were obtained instead.

(12) For related examples, see: (a) Lam, W. W.-L.; Haynes, R. K.; Yeung, L.-L.; Chan, E. W.-K. *Tetrahedron Lett.* **1996**, *37*, 4733–4736. (b) Haynes, R. K.; Au-Yeung, T.-L.; Chan, W.-K.; Lam, W.-L.; Li, Z.-Y.; Yeung, L.-L.; Chan, A. S. C.; Li, P.; Koen, M.; Mitchell, C. R.; Vonwiller, S. C. *Eur. J. Org. Chem.* **2000**, No. 18, 3205–3216.

(13) (a) Xu, Q.; Zhao, C.-Q.; Han, L.-B. *J. Am. Chem. Soc.* **2008**, *130*, 12648–12655. (b) Wang, W.-M.; Liu, L.-J.; Zhao, C.-Q.; Han, L.-B. *Eur. J. Org. Chem.* **2015**, No. 11, 2342–2345.

(14) For an account on optically active *H*-phosphinates, see: Chen, T.; Han, L.-B. *Synlett* **2015**, *26*, 1153–1163.

(15) Martin, J.; Campbell, L. A. Transfer Hydrogenation Process. U.S. Patent 6,696,608, February 24, 2004.

SYNOPSIS

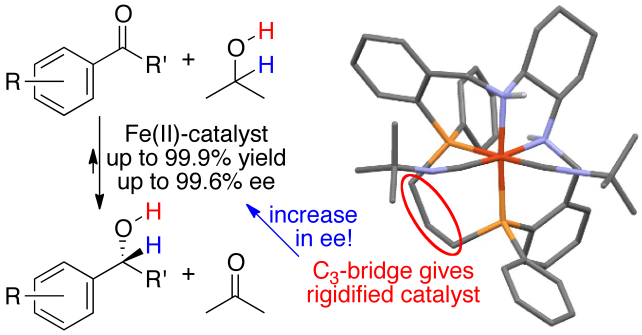
R
R'
+
H
O
H
Fe(II)-catalyst
up to 99.9% yield
up to 99.6% ee
increase
in ee!
C3-bridge gives
rigidified catalyst